ISBN: 978-3-95450-208-0 doi:10.18429/JACoW-IPAC2019-TUPMP036

RESULTS ON THE FCC-hh BEAM SCREEN SAWTOOTH AT THE KIT ELECTRON STORAGE RING KARA*

L. A. Gonzalez, CERN, Geneva, Switzerland
F. Perez, I. Bellafont, ALBA, Barcelona, Spain
V. Baglin, P. Chiggiato, C. Garion, R, Kersevan, CERN, Geneva, Switzerland
S. Casalbuoni, E. Huttel, IBPT-KIT, Karlsruhe, Germany

Abstract

In the framework of the EuroCirCol collaboration [1] (work package 4 "Cryogenic Beam Vacuum System"), the fabrication of the FCC-hh beam screen (BS) prototype has been carried out with the aim of testing it at room temperature on the Karlsruhe Institute of Technology (KIT) 2.5 GeV electron storage ring KARA (KArlsruhe Research Accelerator) light source. The BS prototype was tested on a beamline installed by the collaboration, named as BEam Screen TEstbench EXperiment (BESTEX). KARA has been chosen because its synchrotron radiation (SR) spectrum, photon flux and power match quite well the one foreseen for the 50+50 TeV FCC-hh proton collider. The BS prototype (2 m in length) was manufactured according to the base line design (BD) of the FCC-hh BS. It implements a saw-tooth profile designed to absorb the SR generated at the bending magnets. Also, a laser-ablated anti-electron cloud surface texturing [2] was applied at the BS inner walls. We present here the results obtained at BESTEX and the comparison of the results obtained during irradiation of the saw-tooth profile at different geometric configurations.

INTRODUCTION

The Future Circular hadron Collider (FCC-hh) aims to provide hadron collision at a center of mass of 100 TeV [3]. In such a scenario, proton beams travelling through FCC-hh´s arcs would originate unprecedented levels of Synchrotron Radiation (SR) for hadron machines. Table 1. shows a comparison between the main SR related parameters of LHC and FCC-hh.

SR is known to be at the origin of many detrimental beam effects [4]. In order to preserve the vacuum stability of the machine's vacuum chamber, a novel shaped beam screen (BS) has been designed to minimize the SR related photo-desorption, photo-electron generation and heat load effects at FCC-hh [5].

One FCC-hh BS prototype has been manufactured according to the current BD and tested at the BEam Screen Testbench EXperiment (BESTEX) installed in the 2.5 GeV electron storage ring KARA (KArlsruhe Research Accelerator) light source at the Karlsruhe Institute of Technology (KIT). KARA has been chosen due to its similarities with FCC-hh in terms of SR spectrum, photon flux and power.

Table 1: Comparison between LHC and FCC-hh SR Parameters

SR on BS	LHC	FCC-hh	BESTEX
SR Power [W/m]	0.2	32	32
SR Flux* [ph/m/s]	$4.2\cdot10^{16}$	$1.5\cdot10^{17}$	$4.85\cdot10^{16}$
Critical E [eV]	44.2	$4.3\cdot10^{3}$	$6.2\cdot10^{3}$
Glancing Angle [mrad]	5.06	1.34	18

*Photon Energy above 4eV at nominal operation

EXPERIMENTAL DETAILS

Experimental Setup

BESTEX is an experimental instrument that allows to study SR induced effects on non-leak tight tubular samples under ultra-high vacuum (UHV) [6, 7]. A schematic layout of BESTEX is presented in Fig. 1. The incoming SR can be collimated so that the shape of the incoming photon beam, as well as its photon flux and power, can be tuned. Also, the setup can be pivoted about a vertical axis so as to be able to irradiate at any required glancing angle. Table 1. shows the SR parameters of BESTEX after photon beam collimation in comparison with those for FCC-hh.

A calibrated vacuum Bayard Alpert Gauge (BAG), together with a calibrated residual gas analizer (RGA), is installed at the middle point of the setup. Such configuration allows to measure photo desorption yields from the inner part of the sample under study by using a chimney connection as depicted in Fig. 1.

A water-cooled photon absorber is placed at the back end of the setup. The absorber is equipped with an electrically-insulated electrode on which a positive bias voltage can be applied so as to measure the photo-electrons generated during photon irradiation, and from it derive the fraction of reflected photons.

*The European Circular Energy-Frontier Collider Study (EuroCirCol) project has received funding from the European Union's Horizon 2020 research and innovation programme under grant No 654305. The information herein only reflects the views of its authors and the European Commission is not responsible for any use that may be made of the information.

ISBN: 978-3-95450-208-0 doi:10.18429/JACoW-IPAC2019-TUPMP036

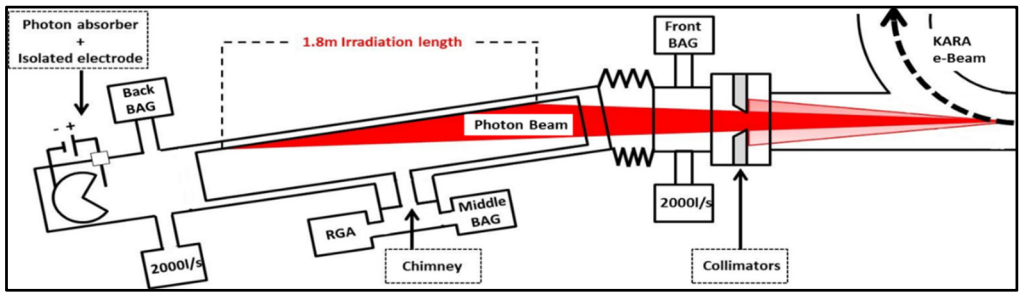

Figure 1: Schematic description of BESTEX.

A more detailed description of the setup can be found elsewhere [6, 7].

Sample

The FCC-hh BS design implements a main chamber (MC) and an antechamber (AC) separated by a slot aperture at the BS's equatorial plane, through which SR travels before impinging on a saw-tooth profile, as in the case of the LHC [8]. A more detailed description of these two designs can be found elsewhere [5, 9].

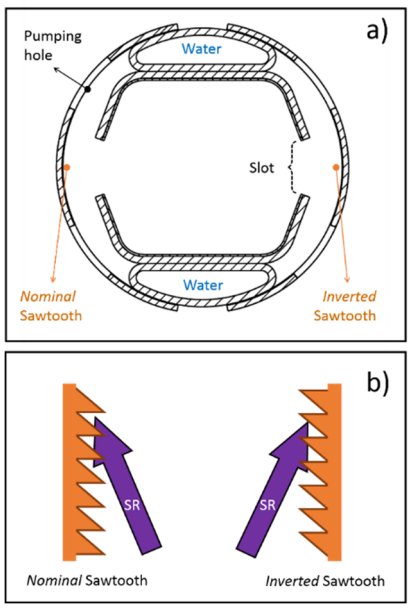

Figure 2: a) Schematic cross section of the FCC-hh BS prototype used in this experiment. b) Graphical descriptions of the different geometrical configurations of both saw-tooth prifiles installed at each side of the BS prototype in which the samples were irradiated.

Figure 2 a shows a cross section of the FCC-hh BS prototype used in this experiment. It has two saw-tooth profiles located at the inner walls of each AC. The saw-tooth profile are LHC-like, with a tooth height of about 40 µm and a longitudinal period of 500 µm as measured at CERN [10, 11]. Recent simulation studies [12] have investigated the effect of irradiating inverted saw-tooth profiles. For this reason, each saw-tooth profile in our sample has been installed in opposite orientations with respect to the incoming photon beam. The teeth of the saw-tooth profile named as nominal are oriented in agreement to the BS base line design as shown in Fig. 2a. The saw-tooth profile installed at the opposite side is named as inverted saw-tooth. As shown in Fig 2b. the photons impinge in a higher glancing angle for the inverted than for the nominal saw-tooth.

Before insertion into BESTEX, the samples were cleaned following standard UHV procedures. Then, after installation, bake out cycles of 24 h at 150 ºC were performed in order to remain within vacuum pressure limits required to operate the storage ring KARA.

During the measurement, the set up was pivoted so as to alternatively irradiate each of the saw-tooth profiles. The nominal saw-tooth was first irradiated up to a dose of $6{\cdot}10^{19}$ ph/m. Then the setup was pivoted to deposit the same dose into the inverted saw-tooth. Such cycle was repeated during the whole experiment. For each cycle the dose applied at each surface was increased in parallel. In such a way, it is possible to simultaneously accumulate photon doses at each of the saw-tooth profiles and minimize the effect of reflected photons towards the opposite saw-tooth profile.

The samples were aligned with respect to KARA's e-beam orbit plane so as to irradiate the intended area with a vertical accuracy of 200 µm.

RESULTS

The log-log plots presented in Fig. 3 show the evolution of the pressure normalized to KARA´s e- beam current as a function of the accumulated dose during irradiation of nominal and inverted saw-tooth.

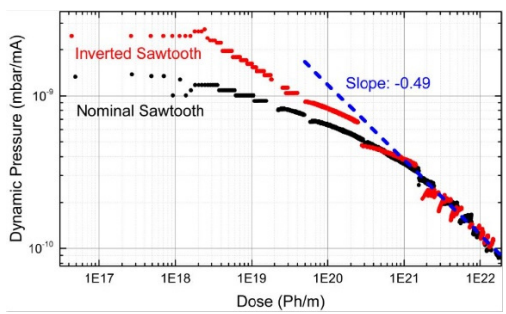

Figure 3: Evolution of the dynamic pressures normalized to the beam current for nominal saw-tooth (black line) and inverted saw-tooth (red line).

At low photon doses, the normalized pressure during irradiation of inverted saw-tooth is about 50% higher than for nominal. A higher amount of reflected photons during

ISBN: 978-3-95450-208-0 doi:10.18429/JACoW-IPAC2019-TUPMP036

irradiation of the inverted saw-tooth, in comparison to nominal the saw-tooth, towards the inner walls of the BS would explain such an effect. Besides, due to the different orientation of each saw-tooth profile with respect to the incoming photon beam, a larger surface is irradiated at more glancing angles in the case of the inverted saw-tooth.

This is also assumed to play an important role in the discrepancy found for the evolution of the dynamic pressure during irradiation of both saw-tooth profiles. At doses of about $1 \cdot 10^{21}$ ph/m, both curves merge into a common value. For higher doses the normalized pressure during irradiation of both saw-tooth profiles evolves with a constant decreasing power-law exponent of -0.49.

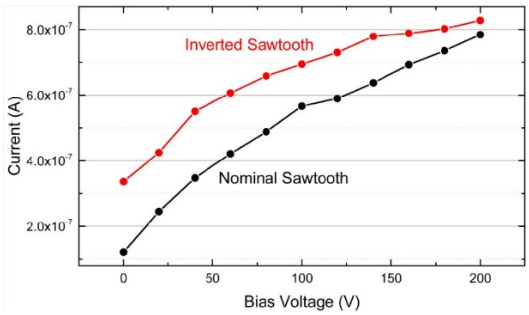

Figure 4: Evolution of the current measured at the photon cup's electrode, normalized to the beam current for Nominal saw-tooth (black line) and Inverted saw-tooth (red line).

Previous experimental findings [12-17] have shown that as the photon dose accumulated on different surfaces increases, the value of the dynamic pressures tend to merge into a common value independently of the nature of the surface under irradiation. Such merging effect takes place at doses around $1 \cdot 10^{23}$ ph/m in all of the cases. It is remarkable in this case that both curves merge at considerably lower doses (2 orders of magnitude) than the value commonly observed at previous experiments. It is however important to take into account that the two surfaces irradiated during this experiment are made of the same material and have been exposed (together) to the same baking and cleaning procedures. Also in both cases the surfaces present a pattern which strongly differs from a flat surface. The latter observations are assumed to be the reason why the two conditioning curves measured in this work merge at lower doses than during irradiation of surfaces of different nature.

In order to investigate the effectiveness of both surfaces in terms of reflectivity, the current of the photo-electrons generated at the photon cup was measured at the photon cup's electrode vs different bias voltages. The plot of Fig. 4 shows the results for inverted and nominal saw-tooth. The photo-electron current was normalized to KARA's electron beam current of 130 mA.

It can be observed that the amount of photons reflected towards the photon cup is clearly larger in the case of the inverted saw-tooth in comparison with the nominal saw-tooth.

For FCC-hh we want to minimize the amount of reflected photons which could contribute to EC at unwanted locations [17]

CONCLUSIONS

The baseline design FCC-hh beam screen prototype was irradiated under similar SR conditions to those of FCC-hh, although at room temperature rather than the 40-60 K temperature interval of the FCC-hh [1]. The evolution of the pressure during irradiation of the BS design shows a constant fitting power-exponent coefficient of -0.49 after an accumulation of $1 \cdot 10^{21}$ ph/m which represents a satisfactory behavior under SR in terms of vacuum performance of FCC-hh [17]. The photoelectron currents measured at the photon cup's electrode indicate that during irradiation of the inverted saw-tooth, a larger amount of photons are reflected towards the inner part of the BS than for the nominal saw-tooth. Such result suggests that for the fabrication of FCC-hh, the nominal orientation of the saw-tooth would be preferable in order to cope with SR in a more efficient way.

Further investigations shall be carried out in order to understand the origin of the apparent discrepancies with previous simulation studies that are found here [12]. For instance, the experimental observation of the reflected photons as a function of the azimuthal angle would allow to quantitatively compare the results obtained in this work with those previously simulated [12].

Future investigation at BESTEX will provide information on the effect of direct irradiation of photons to laser structured surfaces. Such information will be extremely relevant in order to estimate the photo-desorption originated at the BS's main chamber due to irradiation by those photons which are backscattered by the saw-tooth profile.

More importantly, experiments at cryogenic temperatures on several surfaces of relevant interest for the accelerator community are scheduled to be carried out in the near future. Such measurements, as well as those presented in this work, have been and will be used as an input to the montecarlo ray tracing simulations such as those discussed in the companion paper [17].

ACKNOWLEDGEMENTS

This work was carried out within the framework of the EuroCirCol project WP4.6 Measurements on cryogenic beam system prototype. The authors wish to acknowledge the work of the CERN and KARA technician teams.

REFERENCES

[1] https://fcc.web.cern.ch/eurocircol/Pages/default.aspx

[2] M. Benedikt, B. Goddard, D. Schulte, F. Zimmermann, and M. J. Syphers, "FCC-hh Hadron Collider - Parameter Scenarios and Staging Options", in *Proc. 6th Int. Particle Accelerator Conf. (IPAC'15)*, Richmond, VA, USA, May 2015, pp. 2173-2176. doi:10.18429/JACoW-IPAC2015-TUPTY062

ISBN: 978-3-95450-208-0 doi:10.18429/JACoW-IPAC2019-TUPMP036

[3] R. Valizadeh , "Reduction of secondary electron yield for E-cloud mitigation by laser ablation surface engineering", *Appl. Sur. Sci*., vol. 404, pp. 370-379, 2017.

[4] O. Gröbner, "Dynamic outgassing", CERN-OPEN-2000-275, 1999. https://cds.cern.ch/record/455559

[5] F. Perez, "FCC-hh beam vacuum concept (I): BS design, tests and feasibility", in *Proc. FCCweek'18*, Amsterdam, The Netherlands, 2018.

[6] L. A. Gonzalez *et al.*, "Results on the FCC-hh Beam Screen at the KIT Electron Storage Ring KARA", in *Proc. 9th Int. Particle Accelerator Conf. (IPAC'18)*, Vancouver, Canada, Apr.-May 2018, pp. 55-57. doi:10.18429/JACoW-IPAC2018-MOZGBE5

[7] L. A. Gonzalez, "Commissioning of a beam screen test bench experiment (BESTEX) with a FCC-hh type synchrotron radiation beam", unpublished.

[8] O. Gröbner, "Overview of the LHC vacuum system", *Vacuum*, vol. 60, pp. 25-34, 2001.

[9] I. Bellafont *et al*., "Photon tracing and gas-density profiles in the FCC-hh", in *Proc. FCCweek'18*, Amsterdam, The Netherlands, 2018.

[10] I. Bellafont *et al*., "Design of the FCC-hh beam vacuum chamber", to be published.

[11] N. Kos, CERN Rep. LHC-VSS-EC-0010, EDMS Doc. no. 98531, 2004.

[12] G. Guillermo, D. Sagan and F. Zimmermann, "Examining mitigation schemes for synchrotron radiation in high-energy hadron colliders", *Phys. Rev Accel. Beams*, vol. 21, Feb. 2018.

[13] R. Calder *et al*., "Synchrotron radiation induced gas desorption from a Prototype Large Hadron Collider beam screen at cryogenic temperatures", *J. Vac. Sci. Tech. A, vol.* 14, pp. 2618–2623, 1996.

[14] C. Herbeaux *et al*., "Photon stimulated desorption of an unbaked stainless steel chamber by 3.75 keV critical energy photons", *J. Vac. Sci. Tech. A,* vol. 17, pp. 635–643, 1999.

[15] O. Gröbner *et al*., "Gas desorption from an oxygen free high conductivity copper vacuum chamber by synchrotron radiation photons", *J. Vac. Sci. Tech. A,* vol. 12, pp. 846–853, 1994.

[16] C. L. Foerster *et al*., "Desorption measurements of copper and copper alloys for PEP-II", Vacuum, vol. 44, pp. 489 – 49, 1993.

[17] I. Bellafont, R. Kersevan, and L. Mether, "Summary of Modelling Studies on the Beam Induced Vacuum Effects in the FCC-hh", presented at the 10th Int. Particle Accelerator Conf. (IPAC'19), Melbourne, Australia, May 2019, paper TUPMP038, this conference.